The Role of Reactive Oxygen Species in the Biological Activity of Antimicrobial Agents: An Updated Mini Review

P.-L. Lam[a], R. S.-M. Wong[b], K.-H. Lam[a], L.-K. Hung[c], M. Wong[c], L.-H. Yung[c], Y.-W. Ho[d], W.-Y. Wong[a]*, D. K.-P. Hau[e]*, R. Gambari[f,]*, C.-H. Chui[b,c,]*

[a] State Key Laboratory of Chemical Biology and Drug Discovery and Department of Applied Biology and Chemical Technology, The Hong Kong Polytechnic University, Hung Hom, Kowloon, Hong Kong SAR, China.

[b] Department of Medicine and Therapeutics, Prince of Wales Hospital, The Chinese University of Hong Kong, Shatin, NT, Hong Kong SAR, China.

[c] Research and Development Division, KamFord Biotechnology Company Limited, Hong Kong SAR, China.

[d] Allways Health Care Medical Centre, Tsuen Wan, Hong Kong SAR, China.

[e] One Health International Limited, Shatin, Hong Kong SAR, China.

[f] Department of Life Sciences and Biotechnology, Section of Biochemistry and Molecular Biology, University of Ferrara, Ferrara, Italy.

Corresponding authors

W.-Y. Wong, E-mail: wai-yeung.wong@polyu.edu.hk

D. K.-P. Hau, E-mail: desmond.hau@bio-gene.com.hk

R. Gambari, E-mail: gam@unife.it

C.-H. Chui, E-mail: chchui@graduate.hku.hk

Abstract

Antimicrobial resistance remains a serious problem that results in high mortality and increased healthcare costs globally. One of the major issues is that resistant pathogens decrease the efficacy of conventional antimicrobials. Accordingly, discovery and development of novel antimicrobial agents and therapeutic strategies is urgently needed to overcome the challenge of antimicrobial resistance. A potential strategy is to kill pathogenic microorganisms via the formation of reactive oxygen species (ROS). ROS are defined as a number of highly reactive molecules that comprise molecular oxygen (O_2), superoxide anion ($O_2^{\bullet -}$), hydrogen peroxide (H_2O_2) and hydroxyl radicals ($^{\bullet}OH$). ROS exhibit antimicrobial actions against a broad range of pathogens through the induction of oxidative stress, which is an imbalance between ROS and the ability of the antioxidant defence system to detoxify ROS. ROS-dependent oxidative stress can damage cellular macromolecules, including DNA, lipids and proteins. This article reviews the antimicrobial action of ROS, challenges to ROS hypothesis, researches to encourage ROS–mediated antimicrobial lethality, recent developments in antimicrobial agents using ROS as an antimicrobial strategy, safety concerns related to ROS, and future directions in ROS research.

Keywords

Antimicrobial resistance; Oxidative stress; Pathogenic microorganisms; Reactive oxygen species; Safety

1. Introduction

The prevalence of antimicrobial-resistant pathogens is a rising global concern that often results in high mortality rates and increased healthcare costs. Each year at least 2 million persons become infected with antibiotic-resistant bacteria in the United States, leading to at least 23,000 deaths per year [1]. Every year in Europe, approximately 25,000 people and nearly 700,000 in the rest of the world die because of antibiotic-resistant pathogens [2]. Widespread antimicrobial resistance not only triggers a threat to global public health but also compromises the effectiveness of treatment for infectious diseases [3].

The development of antimicrobial resistance is accelerated by misuse and overuse of antibiotics [4], [5]. In 2015, outpatient health care providers in the United States filled more than 269 million antibiotic prescriptions, amounting to 838 antibiotic prescriptions for every 1,000 persons [6]. Overuse and misuse of antibiotics in food-producing animals (i.e., using antibiotics routinely to promote growth and prevent disease in healthy animals [7]) leads to the emergence of antimicrobial-resistant bacteria that are subsequently transferred to humans via food [8]. An estimated 600 million illnesses (almost 1 in 10 people worldwide) occur after eating contaminated food, of whom 420,000 people die every year. Children under 5 years of age account for 40% of the foodborne disease burden, with 125,000 deaths every year [9]. Poor infection prevention and control, as well as a lack of drug discovery and development of potential medications, have also contributed to the antimicrobial-resistance crisis [4], [5]. Therefore, reducing the demand for antimicrobials, advances in novel antimicrobial agents, and development of therapeutic strategies against antimicrobial resistance are potential practices and solutions to the global challenge of antimicrobial resistance [10], [11], [12].

In this respect, an increasing number of researchers have focused on exploring new classes of antimicrobials and the development of novel agents based on existing classes of drugs [13]. Increasing reactive oxygen species (ROS) during antimicrobial therapy represents a novel antimicrobial strategy

because of the associated antimicrobial potency [10]. For example, Surgihoney®, a bioengineered type of honey for wound-healing proposes, manufactured by Healing Honey International, Bicester, Oxfordshire, UK, not only exhibits the antimicrobial effects of honey but also produces high levels of ROS in the form of H_2O_2 [14-16]. This review starts with ROS and oxidative stress in bacterial cells, the antimicrobial action of ROS, challenges to the ROS hypothesis, and work to solidify the ROS–antimicrobial lethality hypothesis, followed by recent developments in ROS-based antimicrobial agents for biomedical uses, and concerns over the safety of ROS as antimicrobials, and finally, future research directions concerning ROS-based antimicrobials.

2. ROS and oxidative stress in bacterial cells

ROS are defined as a number of highly reactive molecules containing molecular oxygen (O_2) [10], [17], [18]. Superoxide anion ($O_2^{\bullet-}$), hydrogen peroxide (H_2O_2) and hydroxyl radicals (•OH) are examples of ROS [17], [18], [19], [20], [21]. $O_2^{\bullet-}$, a primary ROS, is produced by the one-electron reduction of O_2 [18], [22]. H_2O_2 is formed by the reduction of $O_2^{\bullet-}$ via dismutation [18], [22]. •OH is generated from the electron exchange between $O_2^{\bullet-}$ and H_2O_2 via the Harber–Weiss reaction or the reduction of H_2O_2 by the Fenton reaction [18], [22], [23], [24]. Aerobic bacteria require O_2 for respiration or oxidation of nutrients to generate energy. ROS are formed endogenously as in the process of microbial metabolism, and the endogenous ROS formation can be accelerated by exogenous stresses [25], [26], [27]. Highly reactive byproducts of oxygen including $O_2^{\bullet-}$, H_2O_2 and •OH, are formed during the process of aerobic metabolism in cells [26], [27]. The constant formation and detoxification of cellular ROS contribute to a finely controlled and well-balanced redox status in normal cells [27]. However, an imbalance between ROS generation and degradation could appear due to the overproduction of ROS or the deterioration of the antioxidant system. This phenomenon leads to elevations of intracellular ROS levels that exceed cellular tolerance, resulting in oxidative stress [28], [29].

Oxidative stress, caused by ROS, can damage macromolecules, including proteins, DNA, and lipids, resulting in alterations of biological activity, acceleration of mutagenesis, and eventually cell death [21], [27], [30], [31]. To protect cells from the harmfulness of ROS, aerobic bacteria contain enzymes (catalases, superoxide dismutases (SOD), *SodB, SodC, AhpCF, KatG,* and *KatE*) that can detoxify ROS, having regulatory mechanisms (*SoxRS, OxyRS*, and SOS regulons) to counteract the damage [32]. For example, *Escherichia coli* protects itself from oxidative stress by stimulating SOD and catalase activities, which catalyse the dismutation of $O_2^{\bullet-}$ and H_2O_2, respectively. Moreover, regulation of the oxidation response in *E. coli* involves OxyR and SoxRS regulons that transcriptionally regulate catalases and SOD, respectively, in response to H_2O_2 and $O_2^{\bullet-}$ [33], [34], [29]. In contrast, bacterial cells may also use ROS for self-destruction when stress is acute [32], [35], [36].

3. Antimicrobial action of ROS

The ROS-mediated antimicrobial lethality was initially shown by Kohanski et al. in 2007 [37], [38]. The formation of highly deleterious oxidative radical species (•OH) could contribute to the norfloxacin-, ampicillin-, and kanamycin-mediated cell death in *E. coli* and the •OH formation depended on metabolism-related NADH (reduced forms of nicotinamide adenine dinucleotide) depletion, the tricarboxylic acid (TCA) cycle, the electron transport chain, damage to the iron sulphur clusters in proteins, and stimulation of the Fenton reaction [37]. Kohanski et al. in 2008 [39] elucidated the cellular events that connected treatment of bacteria with aminoglycoside antibiotics and the oxidative stress cell death pathway. Aminoglycoside-induced mistranslation and misfolding of membrane-associated proteins activated the envelope two-component stress response sensor, CpxA. Activated CpxA phosphorylated CpxR, which upregulated expression of envelope stress response proteins, such as the periplasmic protease, DegP, in order to protect cells against the increase in misfolded proteins in the

membrane and periplasm. CpxA may also activate the redox-responsive two-component transcription factor, ArcA, and thereby trigger •OH-based cell death.

Wang and Zhao in 2009 [40] extended Collins' findings on the lethal pathway of bactericidal antimicrobials concerning •OH generation or accumulation. The lethality of norfloxacin, ampicillin and kanamycin was 10-fold lower with a *sodA sodB* double mutant. Lethal action of norfloxacin was increased 10–100-fold by a *katG* single mutation or a *katG katE* double mutation, while the sensitivity to killing with ampicillin and kanamycin was increased by an *ahpC* (alkyl hydroperoxide reductase) mutation. In particular, increased superoxide could result in increased peroxide and, ultimately, increased •OH and cell death [37], [40]. Surprisingly, subinhibitory concentrations of superoxide exerted a protective role, as demonstrated by the treatment with plumbagin, a metabolic generator of superoxide, reduce the lethality to *E. coli* by bleomycin, a mutagen and DNA-cleaving agent [41]. Similar observations on the protective effects of *E. coli* from antimicrobials (oxolinic acid, kanamycin, and ampicillin)-mediated killing by subinhibitory doses of plumbagin or paraquat, metabolic generators of superoxide, were further demonstrated by Zhao and co-workers in 2013 [42].

The hypothesis that ROS are associated with antimicrobial-mediated lethality implies that some antimicrobial effects may be unrelated to the primary damage induced by antibiotics [32]. Foti et al. in 2012 [43] reported that ROS contributed to ampicillin- and kanamycin-mediated lethality by oxidization of the guanine nucleotide pool. Incorporation of 8-oxo-guanine derivatives into DNA and RNA stimulated the production of secondary cellular damage, such as double-stranded DNA breaks and misfolding of membrane proteins. This secondary damage caused more ROS and further damage, resulting in cell death. Zhao and co-workers in 2013 [35] solidified the hypothesis of ROS-medicated lethality by providing the first evidence for ROS-mediated post-stress programmed cell death in bacteria. The YihE protein kinase of *E. coli* was found to be a control element for limiting self-destructive response of bacteria to lethal stress. YihE was partially controlled by the Cpx envelope stress-response system,

which, together with MazF toxin and superoxide, had both protective and destructive roles which assist bacteria to decide a live-or-die outcome in response to stress. Inhibition of YihE may provide a novel way to enhance antimicrobial lethality and attenuate virulence.

4. Challenges to the ROS hypothesis

Later, Kohanski's hypothesis in 2007 [37] that ROS contribute to antimicrobial-mediated killing has been criticized even though Wang, Zhao, and co-workers had solidified the work. [32], [44], [45], [46], [47]. Keren et al. in 2013 [44] and Liu & Imlay [45] challenged the idea by Kohanski et al. in 2007 [37] that ROS contributed to antimicrobial-mediated killing. The anaerobic work by Keren et al. in 2013 [44] refused Kohanski's hypothesis. Keren et al. [44] challenged the idea that all antimicrobials killed through ROS-mediated mechanisms by reporting that anaerobiosis inhibited the lethality of the quinolone norfloxacin only at low concentration, that •OH accumulation failed to always correlate with antimicrobial killing, and that dipyridyl, an iron chelator that inhibited the Fenton reaction, and thiourea, a hydroxyl radical scavenger, protected cells from antimicrobial killing under both aerobic and anaerobic conditions. But the choice of norfloxacin showed that Keren et al. actually supported Kohanski et al. because it was expected that inhibition occurred at low concentration of norfloxacin but not at high concentrations, as shown years before by Malik et al. [48], [49]. The effects on anaerobic blockage of killing by quinolones revealed that norfloxacin was a poor choice for ROS studies because it was intermediate in responses [48], [49]. An attenuated killing by bactericidal antibiotics (ampicillin, gentamicin, and norfloxacin) under strict anaerobic conditions has subsequently been confirmed by Dwyer et al. in 2014 [50].

A second study by Liu and Imlay in 2013 [45] raised issues concerning chemical probes of ROS effects. Liu and Imlay's report [45] found that antibiotic treatment did not possess the killing action via the formation of •OH in *E. coli*, as indicated by non-detectable increase in H_2O_2 production after antibiotic

160 treatment. In rebuttal of this argument, Dwyer et al. in 2014 [50] conducted a ROS quantification
161 experiment using a diverse panel of fluorescent reporter dyes to detect different types of ROS in
162 bacteria, including H_2O_2 that could not detected by the previously used 3′-(p-hydroxyphenyl)
163 fluorescein (HPF). Results showed an increase in H_2O_2 production with all bactericidal antibiotics
164 (ampicillin, gentamicin, and norfloxacin). Dwyer et al. also [50] found that antibiotics dynamically
165 affected cellular respiration and induced lethal levels of intracellular H_2O_2. Antioxidants, including
166 oxidative stress defence proteins, could significantly reduce the toxic action of antibiotics, which was
167 highly sensitive to the presence of molecular oxygen. Results showed that environmental factors play a
168 role in killing cells that are physiologically primed for death [50].

169

170 **5. Solidifying the ROS–antibiotic lethality hypothesis**

171 Researchers further solidified the idea of ROS contribution to antibiotics-mediated killing. Metabolomic
172 analysis of *E. coli* after treatment with three different classes of bactericidal antibiotics (beta-lactams,
173 aminoglycosides, quinolones) demonstrated that antibiotic-treated cells exhibited cytotoxic changes
174 indicative of oxidative stress, including higher levels of protein carbonylation, malondialdehyde adducts,
175 nucleotide oxidation, and double-strand DNA breaks [51]. The MalE-LacZ periplasmic-cytoplasmic fusion
176 protein is historically important because of its use in the elucidation of SecY-dependent protein
177 translocation [52]. Interestingly, it has been reported that bacterial cell death caused by the induction of
178 MalE-LacZ [a protein consisting of the NH2-terminal sequences of MalE (periplasmic maltose-binding
179 protein) joined to a modestly NH2-terminally truncated LacZ (β-galactosidase)] [53] did not result
180 directly from jamming of protein translocation or SecY degradation. Rather the experimental findings
181 supported a model in which physiological/metabolic stress from MalE-LacZ expression increased the
182 production of low levels of molecular oxygen and H_2O_2. H_2O_2 did not accumulate to high intracellular

183 levels because cellular conditions favoured its participation in Fenton chemistry, resulting in the
184 oxidization of nucleotides, including 8-oxo-dGTP, which were subsequently incorporated into DNA.
185 Cellular death did not result directly from the incorporation of oxidized nucleotides but rather from
186 lethal DNA problems caused by intermediates of MutM/MutY-dependent base excision repair (BER) [54].

187 Eventually the arguments by Keren et al. [44] and Liu & Imlay [45] were discounted, in part by Hong et al.
188 in 2017 [55] and Luan et al. in 2018 [56], and convincingly by Hong et al. in 2019 [36]. Reports by Keren
189 et al. [44] and Liu & Imlay [45] mainly raised the issues that were i) not enough ROS to actually kill
190 bacterial cells, and ii) no causal relationship between ROS and killing of bacteria by antibiotics, just a
191 correlation. Liu & Imlay [45] argued the Kohanski's hypothesis [37], antibiotic treatment did not
192 accelerate the formation of •OH [44] and H_2O_2 [45]. This was handled by showing that stress could
193 create more sites for ROS attack so very high concentration of ROS might not be necessary [55], [56]. For
194 examples, ROS also took part in thymineless death by converting single-stranded DNA lesions into
195 double-stranded DNA breaks. Involvement of ROS in the terminal phases of thymineless death
196 demonstrated how ROS contributed to stress-medicated bacterial self-destruction [55].

197 It has been criticized that potential off-target effects were difficult to rule out for perturbations with
198 chemical agents, such as thiourea and bipyridyl [25], [45]; thus, statements of causality were
199 questionable when these agents were used. Off-target effects were unlikely with enzymatic suppression
200 of ROS, as when catalase was added to agar or when a catalase deficiency enhanced killing [55], [56].
201 The causal argument could be dealt with by *katG* mutants increasing ROS and increasing killing [56]. The
202 *katG* deficiency, which elevated ROS levels, overcame the protective effect of chloramphenicol,
203 emphasizing the importance of ROS (at moderate, lethal concentrations of nalidixic acid, the *katG*-
204 deficiency-mediated elevation of ROS must be greater than suppression of ROS associated with nalidixic
205 acid-mediated inhibition of protein synthesis) [56].

206 Whether endogenous ROS levels were sufficient enough to kill bacterial cells [25] has been addressed in
207 part by stressors creating lesions that were hypersensitive to ROS attack [50], [55], [56], and the real
208 proof probably came from Hong et al. in 2019, by self-amplification of ROS (intracellular ROS levels were
209 sufficient to kill bacteria once the original inducing stressor was removed) [36]. Hong et al. in 2019 [36],
210 [38] further proposed that ROS-mediated damage, which was secondary to the primary stress-induced
211 lesion, could stimulate a self-amplifying ROS accumulation and thereby cause a self-driven death process
212 in bacteria. Different stressors (ampicillin, nalidixic acid, trimethoprim as well as thermal stress with a
213 *dnaB*-Ts mutant) created potentially lethal primary lesions and stimulated a self-amplifying
214 accumulation of toxic ROS. The latter could be necessary for cell death, as implied by the lethal action of
215 several diverse stressors being halted or reduced by treatment with anti-ROS agents even after removal
216 of the primary stressor. Therefore, bacteria exposed to lethal stressors might not die during treatment
217 in which death could occur after plating on drug-free agar due to poststress ROS-mediated toxicity [36].

218

219 **4. Recent advances in antimicrobial agents using ROS as an antimicrobial strategy for biomedical uses**

220 The antimicrobial resistance crisis has prompted researchers to exert efforts into the development of
221 effective antimicrobial strategies. ROS represent a potential antimicrobial strategy to kill the pathogenic
222 microorganisms. To deal with the emergence of antimicrobial resistance, ROS mediate the lethal action
223 of many antimicrobial agents so that bacterial burden is rapid decreased. Many antimicrobial agents
224 have recently been developed, most of which, such as existing antibiotics, cause bacteria to produce
225 ROS, which resulting in killing of bacteria, while some show synergistic antimicrobial activity with
226 existing antibiotics. Bacteriostatic activity is related to initial lesion formation whereas bactericidal
227 action may result from both primary lesions and the cellular response to primary damage. Focus on the
228 lethal response, rather than on the primary lesion, can be achieved by expressing lethal drug
229 concentrations as a multiple of the minimum inhibitory concentration (MIC) [47]. MIC, related to

230 blocking the growth of microorganisms, measures growth inhibition and resistance [38]. Table 1 shows
231 recent developments in antimicrobial agents using ROS as a potential antimicrobial strategy for
232 biomedical uses.

233

234 Table 1 Recent advances in antimicrobial agents using ROS as a potential antimicrobial strategy for
235 biomedical uses.

Types of antimicrobials	Antimicrobial agents	Microorganisms	Antimicrobial effects related to ROS	Ref.
Natural agents	PT1 and PT2[a] from *Apis mellifera*	*S. aureus*[b]	Antibacterial activity produced by PT1 and PT2, was 2 to 3-fold higher in phenol activity than that of Surgihoney® alone due to the higher H_2O_2 production of the modified honeys.	[15]
	Pyochelin from *Burkholderia paludis*	*E. faecalis*[c] and *S. aureus*	Increased ROS production by pyochelin induced lipid peroxidation and disruption of membrane integrity in *E. faecalis*, resulting in bacterial cell death.	[57]
	PMAP-23[d] from porcine myeloid	*C. albicans*[e]	*C. albicans* treated with 2.5 μM PMAP-23 increased mitochondrial Ca^{2+} overload, NADH oxidation and mitochondrial ROS level. The mitochondrial ROS reduced the glutathione (GSH) level in fungal cells, resulting in oxidative stress and eventually apoptosis.	[58]
	ISO[f] from *Aster yomena*	*C. albicans*	ISO had a synergistic antifungal effect with amphotericin (AmB) and fluconazole (FLC). Combined treatments highly increased intracellular and mitochondrial ROS accumulation in *C. albicans* by > 4 times, resulting in lipid peroxidation, membrane damage, apoptosis and DNA condensation.	[59]
	Apigenin from *Aster yomena*	*C. albicans*	Apigenin (2.5 to 10 μg/mL) reduced the viability of *C. albicans* by 50-80%. Apigenin at 2.5 μg/mL caused mitochondrial dysfunction, mitochondrial calcium overload, mitochondrial ROS accumulation and lipid peroxidation in *C. albicans*.	[60]
	Mo-CBP3-PepI, Mo-CBP3-PepII, and Mo-CBP3-PepIII from *M. oleifera*[g]	*S. aureus*, *B. subtilis*[h], *K. pneumoniae*[i], *E. coli*, *C. albicans*, *C. parapsilosis*[j], *C. krusei*[k], and *C. tropicalis*[l]	*C. parapsilosis* treated with 2.2 μM Mo-CBP3-PepIII, the most potent peptide, showed overproduction of ROS, internalization of propidium iodide, loss of membrane integrity and internal content as well as cell death.	[61]
Synthetic compounds	**HLSn1** and **HLSn2**[m]	*E. coli* and *B. subtilis*	**HLSn1** showed stronger antibacterial activity against *B. subtilis.* The membrane disruption and cytoplasm leakage in *E. coli* might be associated with the ROS generation caused by **HLSn1**.	[62]
	Mononuclear silver(I) [Ag(I)] complexes	*E. coli, P. aeruginosa*[n], *K. pneumoniae, S. aureus, E. faecalis, C. albicans, C. parapsilosis, C. glabrata*[o] and *C. krusei*	Antimicrobial activities of Ag(I) complexes showed comparable antimicrobial activity to silver(I) sulfadiazine (AgSD). On the effect on *C. albicans* SC5314 virulence in epithelial infection model, **1** [$Ag(NO_3$-O,O') (1,7-phen-N7)$_2$] and AgSD showed similar reduction in the hyphal length by 10–15%. **1** was 2-fold higher in cellular ROS generation than that of AmB.	[63]
	Bis-quaternary ammonium salt	*E. coli* and *S. aureus*	Bis-quaternary ammonium salt at 25 μg/mL killed 74% of *E. coli* and 95% of *S. aureus*. Leakage of inner cell contents and detriment of cell membrane in bacteria were caused by Bis-quaternary ammonium salt-induced ROS generation.	[64]
	Cationic heteroleptic iridium(III) [Ir(III)] complexes	*S. mutans*[p] and *S. aureus*	ROS production in human malignant melanoma SK-MEL-28 cells greatly increased after the treatment of photoactivated complexes **3** $[Ir(phen)_2(3,8\text{-dipyrenylphenanthroline})]^{3+}$ and **5** $[Ir(phen)_2(3\text{-pyrenylphenanthroline})]^{3+}$ as compared to dark controls. Significant improvement in antibacterial activity was observed in photoactivated complexes **3** and **5** (EC_{50} = 0.16-0.19 μM) as compared to dark condition (EC_{50} = 1.81-11.2 μM).	[65]

	Cat-Chit[q] film with melanin capsule	*E. coli*, *S. aureus* and MRSA[r]	Cat-Chit film catalyzed transfer of electrons from physiological reductant ascorbate to O_2 for sustained ROS generation, and confered ascorbate-dependent antibacterial activities *in vitro*. In *in vivo* SD rat subcutaneous implantation model, Cat-Chit (reduced with 300 mM ascorbate) had a 2-Log reduction of MRSA number as compared to control Chit and oxidized Cat-Chit surfaces after 3 days.	[66]
	T-TCP micelles composed of TBO grafted CHI and PPS[s]	*L. monocytogenes*[t] and *S. aureus*	T-TCP [equivalent thymol (30 µg/mL) or TCP (300 µg/mL)] with irradiation greatly reduced the biofilms of *L. monocytogenes* and *S. aureus* as compared to T-TCP without irradiation because of large drug release and ROS produced by TBO activation. T-TCP treatment with irradiation damaged almost all of bacterial cells. The cell walls of *S. aureus* became crushed and fragmentary in both T-TCP and TCP treated biofilms under irradiation.	[67]
Nano-materials	CuFe NPs with PG, TEG or PEG 8000[v]	*E. coli*, *B. subtilis* and *S. cerevisiae*[w]	CuFe@PEG8000 displayed the strongest antimicrobial activity against the tested bacteria. Production of intracellular O_2 in *S. cerevisiae* was risen with increasing concentrations of Cu@PEG8000 and CuFe@PEG8000 NPs (12.5 to 100 µg/mL). CuFe@PEG8000 (50 and 100 µg/mL) highly decreased the cell viability of *S. cerevisiae* by > 75% after 5h incubation.	[68]
	Rose Bengal conjugated multiwalled carbon nanotubes (MWCNTs)	*E. coli*	Rose Bengal conjugated MWCNTs (50 µg/mL) with irradiation was significantly toxic to *E.coli* (5.46 log10 reduction in planktonic cells). It induced ~2-fold increase in ROS production in *E. coli* than that of free rose Bengal. It showed > 20% reduction in biofilm formation, cell viability and exopolysaccharide production in *E. coli*, as well as > 20% cellular leakage of protein from *E.coli* as compared to free rose Bengal after radiant exposure.	[69]
	TiO_2DHICA_polym NSs[x]	*E. coli*	Freshly prepared TiO_2DHICA_polym NSs killed > 90% of *E. coli* while NSs after 21 days' storage still killed 50% of bacteria. The antibacterial activity of TiO_2DHICA_polym in the light condition was more than twice times stronger than that in the dark. Significant amounts of OH radicals were generated in TiO_2DHICA polym NSs suspension. TiO_2DHICA polym NSs (200 µg/mL) caused significant disruption of membrane integrity and adhesion of cells on nanostructured aggregate in *E coli.*	[70]
	Rhamnolipid-Ag NPs and Rhamnolipid-Fe_3O_4 NPs[y]	*P. aeruginosa* and *S. aureus*	Both NPs reduced the biofilm formation by >80% during the development of biofilms and after the treatment of pre-formed biofilms as compared to rhamnolipid (<60%). The overall anti-biofilm efficacy of rhamnolipid-Fe_3O_4 NPs was slightly greater than rhamnolipid-Ag NPs (91% vs 88%) due to more ROS release from Fe_3O_4 NPs, which were more toxic to bacterial cells than Ag NPs.	[71]
	Se or Si coated NPs[z]	*P. aeruginosa* and *S. aureus*	Anti-biofilm activity of Se and Si coating for both bacteria was comparable to the cytotoxicity of nanocrystalline silver film. The antibacterial activity of Se and Si NPs might be due to the triggering of ROS abundance (the generation of a singlet oxygen on their surface), causing oxidative damage to bacterial membranes and further death of bacteria.	[72]
	Methylene blue dye conjugated MWCNTs	*E. coli* and *S. aureus*	Photoactivation of methylene blue dye conjugated MWCNTs showed 4.86 log10 reductions in *E. coli* and 5.55 log10 reductions in *S. aureus*, which were > 2 times stronger than free dye. Photoactivated methylene blue dye conjugated MWCNTs reduced the biofilm formation of both bacteria by > 60% as compared to those of non-photoactivated methylene blue dye conjugated MWCNTs (~20 to 30%) and photoactivated dye (~40%). Photoactivated methylene blue dye conjugated MWCNTs highly decreased the viability of bacteria in biofilms by ~50 to 80%; inhibited exopolysaccharide production biofilms by > 40%; as well as induced ~50% of protein leakage after the damage of bacterial cell membranes and > 10 nM/mL of malondialdehyde production by lipid peroxidation.	[73]

[a]Prototype 1 and Prototype 2; [b]*Staphylococcus aureus*; [c]*Enterococcus faecalis*; [d]RIIDLLWRVRRPQKPKFVTVWVR-NH2; [e]*Candida albicans*; [f]isoquercitrin; [g]antimicrobial peptides based on amino acid sequence of *Mo*-CBP_3 (an antimicrobial protein from *Moringa oleifera* seeds); [h]*Bacillus subtilis*; [i]*Klebsiella pneumonia*; [j]*Candida parapsilosis*; [k]*Candida krusei*; [l]*Candida tropicalis*; [m]two novel organotin complexes; [n]*Pseudomonas aeruginosa*; [o]*Candida glabrata*; [p]*Streptococcus mutans*;

[q]catechol-modified chitosan; [r]methicillin-resistant *Staphylococcus aureus*; [s]thymol loaded chitosan micelles composed of toluidine blue O grafted chitosan and poly(propylene sulfide); [t]*Listeria monocytogenes*; [v]copper/iron bimetallic nanoparticles with 1,2-propylene glycol; tetraethylene glycol or polyethylene glycol; [w]*Saccharomyces cerevisiae*; [x]nanostructures synthesized using titanium isopropoxide and 5,6-dihydroxyindole-2-carboxylic acid as precursors of the inorganic and organic phases; [y]rhamnolipid coated silver nanoparticles and rhamnolipid coated iron oxide nanoparticles; and [z]Selenium or silicon coated nanoparticles.

4.1. Natural agents

Cooke et al. [15] examined the antimicrobial activity of Surgihoney® and prototype-modified honeys, Prototype 1 (PT1) and Prototype 2 (PT2) are made by *Apis mellifera* (honeybee) against *S. aureus*. The anti-*S. aureus* activity produced by PT1 and PT2, displayed a 2-fold and almost 3-fold respectively increase in phenol activity when compared with Surgihoney® (31.5%) alone. The two modified honeys, PT1 and PT2, provided higher H_2O_2 production rates (approximately 1 and 1.5 mM H_2O_2, respectively) than Surgihoney® (less than 0.2 mM H_2O_2) over at least 24 h. A striking linear relationship between phenol activity and maximum output of ROS H_2O_2 in modified honeys, SH, PT1 and PT2, was observed. This suggested that the antimicrobial activity of the modified honey samples was highly associated with the production of ROS H_2O_2. These modified honeys would offer an effective and non-toxic dressing that is easy to administer.

Ong et al. [57] extracted an antimicrobial siderophore, pyochelin (Fig. 1), from *Burkholderia paludis* and studied its antimicrobial activity against bacterial strains of *E. faecalis* and *S. aureus*. *Enterococcus* strains (MIC = 3.13 µg/mL) were more susceptible to pyochelin than the *Staphylococcus* strains (MIC = 6.26 µg/mL). *E. faecalis* treated with pyochelin showed a significant increase in intracellular ROS production

when compared to the negative control. Enhanced production of ROS could cause lipid peroxidation that was indicated by an increased malondialdehyde production in *E. faecalis* after 24 h of treatment with 1, 2, and 4 × MICs of pyochelin. The membrane integrity of *E. faecalis* was then disrupted, resulting in bacterial cell death. Survival of *E. faecalis* was significantly decreased by approximately 80% or more when the bacterial cells were treated with 2 × MIC and 4 × MIC of pyochelin after 24 h compared to the negative control. Results revealed that pyochelin might be capable of curing infections caused by *E. faecalis* due to its ability to induce intracellular ROS production in bacterial cells.

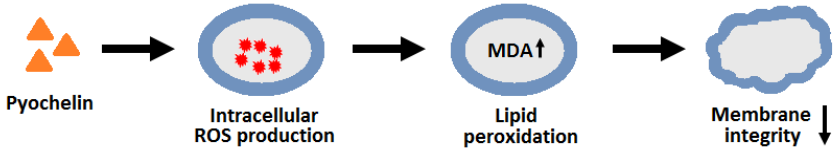

Fig. 1. Antimicrobial mechanism of pyochelin, redrawn from [57].

Kim and Lee [58] studied the anti-candidal activity of PMAP-23 (RIIDLLWRVRRPQKPKFVTVWVR-NH2), an antimicrobial peptide (AMP) derived from porcine myeloid. *C. albicans* cells treated with 2.5 µM PMAP-23 showed a significant elevation of the intracellular Ca^{2+} concentration and mitochondrial Ca^{2+} overload. Disruption of Ca^{2+} homeostasis in *C. albicans* increased NADH oxidation, as indicated by a rapid increase in the ratio of oxidized and reduced forms of nicotinamide adenine dinucleotide (NAD+/NADH). The mitochondrial ROS level was increased by 32% in 2.5 µM PMAP-23-treated cells, as compared to an increase of 14% in untreated cells, revealing that PMAP-23 affected ROS production by inducing mitochondrial Ca^{2+} overload. The overproduction of mitochondrial ROS disrupted the intracellular redox homeostasis in *C. albicans* and reduced the glutathione level in fungal cells, resulting in oxidative stress. Death in 2.5 µM PMAP-23-treated *C. albicans* cells was also indicated by an elevation of the activated metacaspase level (approximately 2 times higher than untreated cells, 30% vs. 13%), an increase in phosphatidylserine (PS) externalization (approximately 2 times higher than untreated cells, (15% vs. 6%), and DNA fragmentation. These findings revealed that PMAP-23 triggered apoptosis in *C. albicans* cells

via mitochondrial Ca^{2+}-induced ROS. The regulation of mitochondrial Ca^{2+} and ROS levels would be a potential target of antifungal treatment.

Kim et al. [59] investigated the synergistic antifungal activity of ISO, one of the phytochemicals isolated from aerial parts of *Aster yomena*, in combination with AmB, FLC and flucytosine (5-FC) against *C. albicans*. ISO was shown to exhibit antifungal activity (MIC = 2.5 μg/mL), while the antifungal effect of AmB, FLC and 5-FC was associated with a MIC value of 1.3 μg/mL. The fractional inhibitory concentration index (FICI) confirmed that AmB and FLC were synergistic with ISO, with FICIs < 0.5. The individual MIC values for the combination of ISO/AmB and ISO/FLC were 0.31/0.16 μg/mL and 0.31/0.33 μg/mL, respectively. ISO, AmB and FLC also increased the intracellular ROS accumulation in *C. albicans* by 24%, 6% and 13% when compared with untreated cells. The intracellular and mitochondrial ROS accumulation in *C. albicans* occurred synergistically, with a significant increase in ROS generation for the combinations of ISO, AmB, and FLC. The activity of superoxide dismutase (SOD, as a ROS-scavenging enzyme) was found to be significantly reduced in ISO/AmB and ISO/FLC, respectively, suggesting that a disruption of the normal oxidative process and a dysfunction of the antioxidant system occurred. Combinations of ISO with AmB and FLC greatly increased the malondialdehyde level in *C. albicans*. However, increased levels of lipid peroxidation in fungal cells caused by the combined treatments were reversed by the pretreatment with *N* - acetylcysteine (NAC). These results demonstrated that lipid peroxidation resulted from ROS accumulation in response to the combined treatments. Although ISO/AmB and ISO/FLC treatments could trigger cell death, the ISO/FLC showed a significant increase in cell death and DNA condensation when compared with ISO alone. The level of membrane damage in fungal cells exposed to the combined treatments (ISO/AmB and ISO/FLC) significantly increased compared with the control and ISO alone. These results demonstrated that ISO could be used with conventional antifungal agents for the treatment of fungal infections.

Lee et al. [60] isolated apigenin (Fig. 2) from the aerial parts of *Aster yomena*, a perennial herb that grows mainly in South Korea, and examined its antifungal properties against *C. albicans*. Apigenin significantly inhibited the growth of *C. albicans* by approximately 50 to 80% at high concentrations (2.5, 5, and 10 μg/mL), whereas crude extract did not show any effect when used at the same concentration. Apigenin could reduce the survival of fungal cells even at 1/2 MIC (2.5 μg/mL), compared to the crude extract. Apigenin disrupted intracellular ion homeostasis of *C. albicans* strains at sub-MIC (2.5 μg/mL), as indicated by significant increases in potassium leakage and calcium ion levels in the mitochondria compared with the untreated control. Apigenin also induced mitochondrial dysfunction in *C. albicans*. Mitochondrial change was indicated by the significantly decreased ratio of FL2/ FL1 fluorescence in apigenin-treated cells and the significantly increase in mitochondrial mass change of apigenin-treated cells measured via Mitotracker Green staining when compared with untreated cells. MitoSOX Red fluorescence intensity after apigenin treatment significantly increased by 66% as compared to that in untreated cells (21%), revealing that apigenin treatment increased ROS accumulation in the mitochondria. These results demonstrated that apigenin disrupted the mitochondrial membrane potential, resulting in mitochondrial dysfunction. Apigenin-induced mitochondrial calcium overload resulted in ROS accumulation inside mitochondria, as indicated by an increase in H_2DCFDA fluorescence intensity of apigenin (45%) when compared with cells pre-treated with ruthenium red (RR, used as a mitochondrial calcium uptake inhibitor) (24%). Fungal cells treated with apigenin showed a significant decrease in reduced the glutathione/glutathione disulphide (GSH/GSSG) ratio compared with untreated and RR-pre-treated cells. Apigenin treatment led to a calcium signalling dependent increase in GSSG relative to GSH, suggesting oxidative stress to the cells. High levels of malondialdehyde were shown in cells treated with apigenin when compared to the untreated and RR-pretreated cells. These findings revealed that apigenin led to oxidative damage to intracellular lipids, and the inhibition of mitochondrial calcium overload reduced apigenin-induced lipid peroxidation. These results suggested that apigenin-

induced ROS accumulation disrupted intracellular redox states and was mediated by mitochondrial calcium signalling modulated by ROS generation. Apigenin-induced apoptosis in *C. albicans* was more directly associated with mitochondrial calcium overload than ROS generation, as indicated by the significant counteraction of apigenin-induced effects on metacaspase activity by RR pretreatment. RR pretreatment significantly attenuated the apigenin-induced metacaspase activity (38%) by approximately 10% when compared with NAC (used as ROS scavenger) pretreatment (approximately 3%).

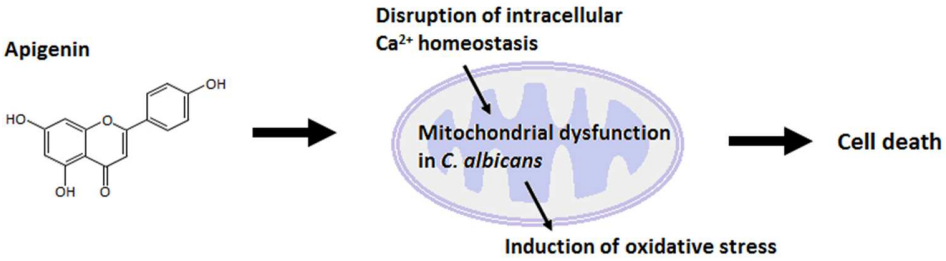

Fig. 2. Antimicrobial mechanism of apigenin, redrawn from [60].

Oliveira et al. [61] designed and synthesized the antimicrobial peptides (*Mo*-CBP$_3$-PepI, *Mo*-CBP$_3$-PepII, and *Mo*-CBP$_3$-PepIII) based on the amino acid sequence of *Mo*-CBP$_3$, an antimicrobial protein from *Moringa oleifera* seeds. The antimicrobial activity of synthesized peptides was examined *in vitro* against *S. aureus* and *B. subtilis* and the Gram-negative bacteria *K. pneumoniae* and *E. coli*, as well as the fungal pathogens *C. albicans*, *C. parapsilosis*, *C. krusei*, and *C. tropicalis*. Among the peptides, *Mo*-CBP$_3$-PepIII was the most potent peptide against *S. aureus* (MIC$_{50}$ = 4.4 µM) and *Candida* spp. (MIC$_{50}$ ranged from 2.2 to 17.5 µM). *C. parapsilosis* was selected to establish the mode of anticandidal action. The fungal cells treated with 2.2 µM *Mo*-CBP$_3$-PepIII showed an overproduction of ROS and internalization of propidium iodide. The SEM analysis further revealed the loss of membrane integrity in the *C. parapsilosis* cells, resulting in internal content loss and cell death. In contrast, three peptides at 280 µM did not lead to haemolysis of human erythrocytes. The most active antimicrobial peptide, Mo-CBP3-

PepIII, did not show cytotoxicity to Vero cells up to 72 h of incubation even at a concentration 64 times higher than the MIC_{50} value calculated for *S. aureus* (4.4 μM), 127 times higher than the MIC_{50} values for *C. albicans C. parapsilosis, and C. krusei* (2.2 μM), and 16 times higher than the MIC_{50} value for *C. tropicalis* (17.5 μM). Therefore, *Mo*-CBP_3-PepIII would be a promising candidate for the development of a new antimicrobial agent for clinical application.

4.2. Synthetic compounds and substances

Hu et al. [62] synthesized two novel organotin complexes (**HLSn1** and **HLSn2,** Fig. 3) and investigated the potential antibacterial activity of the complexes. Both complexes showed stronger antibacterial activity than the ligand **HL** against *E. coli* and *B. subtilis* because of the effect of the Sn atom. **HLSn1** exerted a slightly stronger antibacterial activity in comparison with **HLSn2** because of the high lipophilicity of **HLSn1** with the flexible alkyl chains and ease of absorption by the bacterial membrane, resulting in damage to the bacterial membrane. Complex **HLSn1** was more efficient at inhibiting the growth of *B. subtilis*, with a lower MIC 90% of 2 μg/mL than kanamycin (8 μg/mL) and a larger inhibition zone of 18 mm than kanamycin (6 mm). An insignificant cytotoxic effect on the human embryonic lung fibroblast (HELF) cells was found even upon increasing the concentration of **HLSn1** to 10 μg/mL during a 24-h incubation The super-resolution imaging results showed that complex **HLSn1** was tightly adsorbed around the cell walls of *E. coli* and even entered the cells. The SEM images also demonstrated that most cells suffered from membrane disruption and cytoplasm leakage after **HLSn1** treatment for 2 h. Remarkable fluorescence was detected in *B. subtilis* and *E. coli* in the presence of complex **HLSn1**, whereas no fluorescence was observed in the absence of the complex. An exorbitant level of ROS could enhance the oxidative stress in cells, which could destroy the bacterial membrane and lead to cell death. Results revealed that the generation of ROS and subsequent membrane destruction might be the primary mechanism of the antimicrobial function. Complex **HLSn1** would be a useful tool for further

applications in the super-resolution bacteria imaging, diagnostics, and the treatment of bacterial infectious diseases.

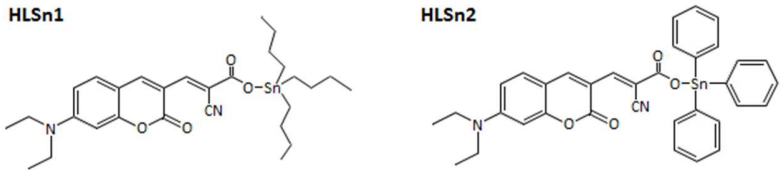

Fig. 3. Chemical structure of **HLSn1** and **HLSn2**, redrawn from [62].

Savić et al. [63] synthesized mononuclear Ag(I) complexes with 1,7-phen, [Ag(NO_3-O,O′) (1,7-phen-N7)$_2$] (**1**) and [Ag(1,7-phen-N7)$_2$]X, X = ClO_4− (**2**), CF_3SO_3− (**3**), BF_4− (**4**) and SbF_6− (**5**) (Fig. 4). Their potential antimicrobial activities were tested on five bacterial strains, including Gram-negative *E. coli*, *P. aeruginosa*, *K. pneumoniae*, and Gram-positive *S. aureus* and *E. faecalis*, as well as four Candida spp. (*C. albicans, C. parapsilosis, C. glabrata* and *C. krusei*). Ag(I) complexes showed comparable antibacterial activity (MIC values between 25 and 125 μM) when compared with silver(I) sulfadiazine (AgSD) (MIC values between 25 and 100 μM). The antifungal activity of the complexes was either comparable to or stronger than AgSD (MIC = 1.2 to 11.3 μM vs. 2.5 to 10 μM). The cytotoxicity of the complexes against healthy human fibroblast MRC5 cells (IC_{50} = 12.5 to 40 μM) was lower than AgSD (IC_{50} = 10 μM). Complex **1** displayed a 5-fold lower MIC value against *C. albicans* (MIC = 1.8 μM) and 4-fold lower cytotoxicity (IC_{50} = 40 μM) compared to AgSD. Concerning the effect on *C. albicans* SC5314 virulence in an epithelial infection model, complex **1** and AgSD showed similar reductions of hyphal length by 10–15% in comparison to the untreated control. However, complex **1** demonstrated a greater reduction of epithelial damage than AgSD. Complex **1** showed a 2-fold higher generation of cellular ROS after a 1.5-h incubation when compared with AmB, a clinically used antifungal drug. The molecular docking results revealed that DNA might not be the primary target of complex **1** within *Candida* cells; however, it might be one of the biomolecules with which this Ag(I) complex interacted. Complex **1** showed 1.2-fold lower

toxicity to zebrafish embryos [the concentration causing a lethal effect at 50% (LC_{50}) = 5.89 µM] than AgSD (LC_{50} = 5.02 µM). Complex **1** did not show cardiotoxicity to zebrafish embryos in contrast to AgSD. Complex **1** did not significantly elevate ROS production in zebrafish embryos even at the 6 × MIC dose compared to the untreated control, whereas AgSD treatment significantly increased ROS in embryos at the MIC dose when compared with the control group. Ag(I) complex **1** exhibited antifungal potency and favourable pharmacological properties; it was more effective and safe than the clinically used AgSD.

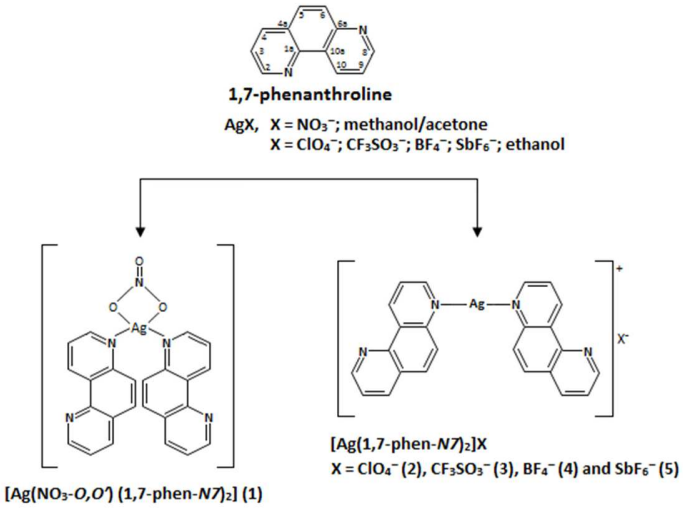

Fig. 4. Chemical structure of Ag(I) complexes with 1,7-phen, redrawn from [63].

Song et al. [64] synthesized a long-chain high-molecular organic bis-quaternary ammonium salt and investigated its antibacterial activity against *E. coli* and *S. aureus*. The MIC values of bis-quaternary ammonium salt against *E. coli* and *S. aureus* ranged from 16 to 64 µg/mL and 8 to 32 µg/mL, respectively. Bacterial death gradually increased with an increasing concentration of bis-quaternary ammonium salt, from below 40% at 12.5 µg/mL to over 99% at 200 µg/mL. Bis-quaternary ammonium salt at 25 µg/mL showed a much stronger inhibitory effect on bacterial growth. Bis-quaternary ammonium salt at 25 µg/mL inhibited 74% of *E. coli* and 95% of *S. aureus,* whereas CTAB (positive control) only killed 55% of *E. coli* and 50% of *S. aureus* at the same concentration. The scanning electron microscope (SEM) and transmission electron microscopy (TEM) analyses confirmed that morphological changes occurred in

both *E. coli* and *S. aureus* treated with 200 μg/mL BQAS, as indicated by crumpled and collapsed cell walls in SEM images and blurred cell walls or partially dissolved edges of cell walls in TEM images. Significant rise in leaked proteins in bacteria verified the damage to the bacterial cell membrane due to the direct contact of the bacteria with bis-quaternary ammonium salt. Bis-quaternary ammonium salt had a highly positive surface charge (ζ-potential ca. +30.2 mV) and could lead to strong contact with the bacterial membrane. The leakage of the inner cell contents revealed that the exposure of bacteria to bis-quaternary ammonium salt induced ROS generation and had a detrimental effect on the cell membrane. The level of ROS generation increased with the increasing concentration of bis-quaternary ammonium salt, as demonstrated by a stronger green fluorescence intensity of *E. coli* and *S. aureus* during treatment with 200 μg/mL bis-quaternary ammonium salt, representing a 5.5 and 4.1 times greater level than in the control group. Moreover, bis-quaternary ammonium salt showed no obvious cytotoxicity on the proliferation of mouse breast cancer 4T1 cells within the concentration of 50 μg/mL, with approximately 90% cell viability. These results suggested that bis-quaternary ammonium salt could be a potential candidate for antibacterial therapy against bacterial infections.

Wang et al. [65] synthesized a series of cationic heteroleptic ir(III) complexes bearing tris-diimine ligands $[Ir(phen)_2(R\text{-}phen)]^{3+}$ [R-phen = phenanthroline (**1**), 3,8-diphenylphenanthroline (**2**), 3,8-dipyrenylphenanthroline (**3**), 3-phenylphenanthroline (**4**), 3-pyrenylphenanthroline (**5**), and 3,8-diphenylethynylphenanthroline (**6**)] (Fig. 5), and their *in vitro* photobiological activities were studied. Among the complexes, complexes **3** and **5** had singlet oxygen quantum yields as high as 81 and 72%, respectively. These complexes possessed long-lived triplet excited states (ca. 4.3 – 33 *μs*), which facilitated bimolecular interactions with ground-state oxygen for high ROS production. Treatment of human malignant melanoma SK-MEL-28 cells with both complexes **3** and **5** substantially increased ROS production upon photoactivation with 50 J cm^{-1} visible light when compared with the dark controls and the positive control tert-butyl hydrogen peroxide TBHP. Photoactivated complexes **3** and **5** showed

significant improvements in antibacterial activity against *S. mutans* and *S. aureus*, with mean EC_{50} values of 0.18 µM vs 0.19 µM for *S. mutans* and 0.17 µM vs 0.16 µM for *S. aureus*, compared to the dark condition (mean EC_{50} = 11.2 vs 2.87 for *S. mutans* and 1.81 vs 5.59 µM vs 0.16 µM for *S. aureus*). These complexes could act as light-responsive agents against bacterial cells, possibly via mechanisms such as the generation of ROS.

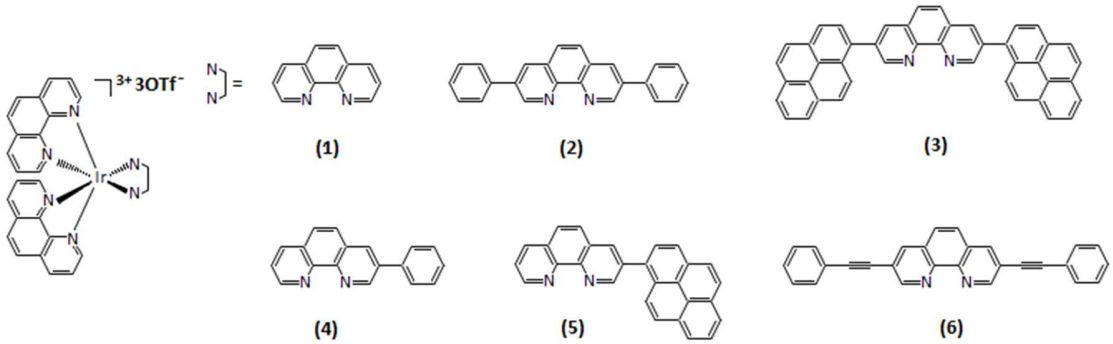

Fig. 5. Chemical structure of complexes **1** – **6**, redrawn from [65].

Liu et al. [66] prepared a catechol-modified chitosan (Cat-Chit) film that imitated features of the melanin capsule generated during an insect immune response to infection. The *in vitro* antimicrobial activity and *in vivo* wound healing efficacy of Cat-Chit film were examined. Cat-Chit film was shown to catalyse the transfer of electrons from the physiological reductant ascorbate to O_2 for sustained ROS generation, and to confer ascorbate-dependent antimicrobial activities against *E. coli*, *S. aureus* and MRSA *in vitro*. Unmodified control Chit, oxidized Cat-Chit films and reduced Cat-Chit films treated with 1 and 10 mM ascorbate did not show any cytotoxicity towards HaCaT cells, while the films treated with 300 mM ascorbate slightly decreased cell viability by 15%. In an *in vivo* rat subcutaneous implantation model, Cat-Chit (reduced with 300 mM ascorbate) showed an average 2-Log reduction of the MRSA number on the film surface in comparison to the control Chit and oxidized Cat-Chit surfaces after 3 days. The *in vivo* mouse excisional wound splinting model also demonstrated that the wound treated with the Cat-Chit film (reduced with 10 mM ascorbate) showed significantly higher closure with complete formation of

new epithelium, development of more blood vessels and hair follicles as well as regeneration of more uniformly distributed collagen, compared to those treated with Chit and oxidized Cat-Chit groups with significant inflammatory cell infiltration on day 14. Wounds treated with reduced Cat-Chit film were statistically reduced in the bacterial population than other groups, which was consistent with the film possessing *in vitro* antimicrobial activity. Reduced Cat-Chit film could offer potential for wound management by protecting against pathogen infection via the generation of antimicrobial ROS.

Wang et al. [67] fabricated light-responsive T-TCP, which were prepared via self-assembly by an amphiphilic copolymer consisting of TBO as an ROS generator for the light-activated antimicrobial photosensitizer) grafted CHI (CHI-TBO) and PPS for the treatment of bacterial biofilms. TBO-CHI-PPS showed a significant increase in fluorescence intensity of singlet oxygen sensor green (SOSG) (approximately 4 times higher than TBO-CHI-PPS without irradiation) upon the irradiation using the 670 nm light source (20 mW/cm^2, 10 min), whereas the fluorescence intensity of SOSG in TBO-CHI-PPS without irradiation remained at the original level. The transmittance of TBO-CHI-PPS with irradiation also greatly increased from 5 to 57%. These results confirmed that TBO-CHI-PPS hydrophobicity-hydrophilicity transition was caused by ROS generated under irradiation (by TBO) because of the oxidation of hydrophobic thioether to hydrophilic sulfoxide or sulfone. T-TCP [equivalent thymol (30 μg/mL) or TCP (300 μg/mL)] with irradiation significantly reduced the biofilms of *L. monocytogenes* and *S. aureus* when compared with T-TCP without irradiation due to the large drug release and portion of ROS produced by TBO activation. Almost all bacterial cells were destroyed in T-TCP treatment under irradiation. The cell walls of *S. aureus* became crushed and fragmentary in both T-TCP and TCP treated biofilms under irradiation, whereas both control and thymol-treated biofilms displayed intact bacterial cells with a round shape and a highly organized and well-defined architecture even under irradiation. This formulated TCP could be useful for other hydrophobic antibacterial agents as a controllable topical disinfectant.

482

483

484

485 **4.3. Nanomaterials**

486 Antonoglou et al. [68] synthesized CuFe NPs when three types of polyols, including PG, tetraethylene
487 TEG and PEG 8000 (M1-M3 samples, respectively) directly reacted with $Fe(NO_3)_3 \cdot 9H_2O$ and
488 $Cu(NO_3)_2 \cdot 3H_2O$ under solvothermal conditions inside an autoclave, in a hybrid polyol process. The
489 antimicrobial activity of CuFe NPs was examined. The CuFe@PEG8000 (M3) showed the strongest
490 antimicrobial activity, with a half-minimal inhibitory concentration (IC_{50}) of 6.3 μg/mL for *E. coli*; 7.8
491 μg/mL for *B. subtilis* and 34.34 μg/mL for *S. cerevisiae* when compared with other NPs (IC_{50} ranging from
492 7.9 to 98.9 μg/mL). To further study the collective effects of Cu and Fe, the intracellular and extracellular
493 ROS generated during the incubation of *S. cerevisiae* cultures with CuFe and Cu NPs were measured.
494 Production of intracellular O_2 increased with increasing concentrations of NPs (12.5, 25, 50 and 100
495 μg/mL of NPs) whereas no extracellular O_2 was detected, suggesting that both CuFe and Cu NPs entered
496 the fungal cells during the incubation. *S. cerevisiae* treated with high concentrations (50 and 100 μg/mL)
497 of CuFe@PEG8000 (M3) showed less than 25% cell viability after a 5-h incubation.

498 Anju et al. [69] synthesized rose Bengal conjugated MWCNTs and studied their antimicrobial
499 photodynamic activity against *E. coli*. The 50 μg/mL rose Bengal conjugated MWCNTs showed
500 significantly higher photo toxicity to *E.coli* (5.46 log10 reduction in planktonic cells) than free rose
501 Bengal (3.56 log10 reduction) at the same concentration after a 24-h incubation when irradiated for
502 10 min using a 50 mW green laser with an energy fluence rate of 1674.7 J/cm^2. The total amount of ROS
503 produced by the rose Bengal conjugated MWCNTs (50 μg/mL) in *E. coli* was approximately 2 times
504 higher than the free rose Bengal at the same concentration. Rose Bengal conjugated MWCNTs at

505 50 μg/mL also showed more than a 20% reduction in biofilm formation of *E. coli*, the number of viable
506 cells of *E. coli* and exopolysaccharide production in *E. coli*, as well as more than 20% cellular leakage of
507 protein from *E. coli* when compared with free rose Bengal (50 μg/mL) after radiant exposure.
508 Overproduction of ROS could enhance photo destruction of both planktonic cells and biofilms of *E. coli*.
509 Rose Bengal conjugated MWCNTs-treated samples (irradiated) displayed lower intensity of DNA bands
510 when compared with non-irradiated samples. Rose Bengal conjugated MWCNTs could be used to
511 control infections induced by *E. coli* after combining with the photodynamic therapy due to the increase
512 in ROS production inside the bacterial cells.

513 Vitiello et al. [70] prepared the hybrid TiO_2DHICA_polym NSs (Fig. 6) by hydrothermal synthesis, by using
514 titanium isopropoxide and 5,6-dihydroxyindole-2-carboxylic acid as precursors of the inorganic and
515 organic phases, respectively. The antibacterial activity of the TiO_2DHICA_polym NSs (0–400 μg/mL) was
516 tested on the Gram-negative bacteria *E. coli*. A quick dose-dependent biocide action occurred as early as
517 10 min following the incubation of *E. coli* with TiO_2DHICA_polym NSs. The freshly prepared
518 TiO_2DHICA_polym NSs killed more than 90% of the bacterial cells, while NSs after 21 days of storage still
519 induced approximately 50% bacterial mortality. The antibacterial action of TiO_2DHICA_polym under light
520 conditions was more than two times stronger than in the dark. The EPR spectra of DHICA–eumelanin
521 and TiO_2DHICA_polym NSs demonstrated a characteristic quartet with a 1 : 2 : 2 : 1 intensity ratio
522 corresponding to the DMPO–OH adduct formed from the trapping of OH radical on DMPO whereas no
523 signals were observed in both DMPO aqueous solution and bare TiO_2 NSs in aqueous suspension. The
524 results confirmed that significant amounts of OH radicals were formed in DHICA–eumelanin and
525 TiO_2DHICA polym NSs suspensions. A decrease in OH production was observed from day 0 to day 21 in
526 the case of TiO_2DHICA_polym stored under environment light, corresponding to the exerted
527 antibacterial activity. TiO_2DHICA_polym NSs contained a higher number of carboxylic groups, which
528 increased the number of hydrogen bonds with lipid head groups, thus improving the affinity and binding

to bacterial membranes. Optical images revealed a significant disruption of membrane integrity and adhesion of cells on nanostructured aggregates in bacterial cells treated with 200 µg/mL TiO_2DHICA_polym for 10 min. No cytotoxic effects were detected in HaCaT cells treated with TiO_2DHICA_polym at various concentrations (from 0 to 800 mg/mL) for 24 h. This study could be useful for the development of eumelanin-based systems with enhanced activity against drug-resistant pathogens.

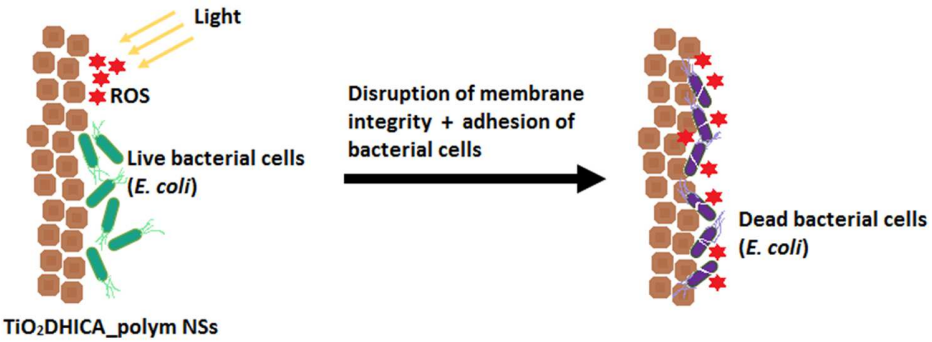

Fig. 6. Antimicrobial mechanism of TiO_2DHICA_polym NSs, redrawn from [70].

Khalid et al. [71] prepared rhamnolipid-Ag NPs and rhamnolipid-Fe_3O_4 NPs and studied their synergistic antibacterial and anti-adhesive properties against biofilms formed by *P. aeruginosa* and *S. aureus*. The effective concentration of rhamnolipid-coated NPs was 1 mg/mL against *P. aeruginosa* and *S. aureus*, and *S. aureus* was 5 times more susceptible than *P. aeruginosa* to the treatment. Rhamnolipid-coated NPs (1 mg/mL) were able to inhibit the growth of developing biofilms and to treat the pre-formed biofilms of *P. aeruginosa* and *S. aureus*. The anti-biofilm activity of rhamnolipid-coated NPs (1 mg/mL) was much stronger than the 10% rhamnolipid (1 mg/mL). Both rhamnolipid-Fe_3O_4 NPs and rhamnolipid-Ag NPs showed more than 80% of biofilm inhibition during the development of biofilms and after the treatment of pre-formed biofilms when compared with rhamnolipid (less than 60%). The overall anti-biofilm efficacy of rhamnolipid-Fe_3O_4 NPs was slightly higher than rhamnolipid-Ag NPs (91% vs 88%), suggesting a greater release of ROS by Fe_3O_4 NPs, demonstrating greater toxicity to the bacterial cells

548 than Ag NPs. The ROS produced by Fe_3O_4 NPs induced oxidative damage to the cells resulting in a loss of
549 their physiology. The microscopic analysis of biofilms treated with rhamnolipid-coated NPs for 24–48 h
550 confirmed that the biofilm architecture was altered and the distribution of viable bacteria was
551 significantly reduced. Rhamnolipid-coated Ag and Fe_3O_4 NPs could be more efficient and cost-effective
552 than using rhamnolipid alone for antibacterial and anti-biofilm applications. They could also be used as
553 efficient drug carriers and in non-woven bioresorbable dressings containing active compounds to treat
554 localized chronic wounds.

555 Nastulyavichus et al. [72] prepared Se and Si NPs with high-purity -based coatings by rapid and effective
556 nanosecond laser ablation of the corresponding solids in water and tested their antibacterial properties
557 towards *S. aureus* and *P. aeruginosa*. Se and Si coating strongly inhibited biofilm formation for both
558 bacteria, which was comparable to the cytotoxicity of the nanocrystalline silver film. The antibacterial
559 activity of Se and Si NPs might be related to the triggering of ROS abundance (the generation of a singlet
560 oxygen on their surface), resulting in oxidative damage to bacterial membranes and further bacterial
561 death.

562 Parasuraman et al. [73] investigated the antibacterial and anti-biofilm properties of methylene blue dye
563 conjugated MWCNTs against *E. coli* and *S. aureus* using a laser light source at 670 nm with radiant
564 exposure of 58.49 J/cm^2. The binding of free dye to the bacteria was lower than methylene blue dye
565 conjugated MWCNTs. The maximum uptake levels of methylene blue dye conjugated MWCNTs at 90
566 min were increased by approximately 10% and more than 20% for *E. coli* and *S. aureus*, respectively,
567 when compared with the free dye. Photoactivation of methylene blue dye conjugated MWCNTs
568 displayed 4.86 ± 0.93 log10 reductions in *E. coli* and 5.55 ± 0.43 log10 reductions in *S. aureus*, which
569 were more than 2 times stronger than the free dye. Methylene blue dye conjugated MWCNTs
570 significantly increased intracellular ROS production in both irradiated strains compared to non-irradiated

cells treated with methylene blue dye conjugated MWCNTs and methylene blue dye as well as irradiated cells treated with methylene blue dye. Photoactivated methylene blue dye conjugated MWCNTs also demonstrated a much better anti-biofilm effect when compared with others. A greater than 60% reduction in biofilm formation of both strains was detected in the photoactivated methylene blue dye conjugated MWCNTs, which was significantly higher than those of non-photoactivated methylene blue dye conjugated MWCNTs (~30% for *S. aureus* and ~20% for *E. coli*) and photoactivated methylene blue dye (~40% for both strains). The viabilities of cells treated with photoactivated methylene blue dye conjugated MWCNTs were significantly reduced by ~50% and ~80% in *E. coli* and *S. aureus* biofilms, respectively. Photoactivated methylene blue dye conjugated MWCNTs caused exopolysaccharide production in *E. coli* and *S. aureus* biofilms was inhibited by more than 40%, whereas exopolysaccharide production was inhibited by only 30% or below in both strains treated with methylene blue dye. Approximately 50% of proteins leaked after the bacterial cell membrane damage by methylene blue dye conjugated MWCNTs, and significantly high levels of malondialdehyde produced by lipid peroxidation in *E. coli* (11.33 nM/mL) and *S. aureus* (12.69 nM/mL) were detected after the treatment with photoactivated methylene blue dye conjugated MWCNTs. MWCNTs would be an efficient carrier for methylene blue dye to enhance the photodynamic treatment in the fight against antibiotic resistant bacterial strains.

5. Safety concerns for ROS as an antimicrobial agent

Considering their potency in causing microbial toxicity, ROS are widely used as a potential antimicrobial strategy against a broad range of microbial pathogens. Treatments with high concentrations of ROS generally result in powerful and effective microbicidal action. However, the risk of potential toxicity to healthy cells and tissues is expected to be increased and should be carefully considered. In fact, ROS as a topical antimicrobial agent might induce adverse effects to the skin. Skin is vulnerable to the damage

promoted by ROS, being rich in unsaturated fatty acids and exposed to high oxygen stress induced by ROS. ROS, especially the hydroxyl radical, induces oxidative damage to biological macromolecules such as DNA, carbohydrates, lipids and proteins. Among the most susceptible targets are polyunsaturated fatty acids, for which the initiation of lipid peroxidation is induced by ROS. Oxidative damage to membrane lipids in cells can attack cellular components and ultimately lead to cell death [74]. Intracellular ROS production was found to be proportional to cytotoxicity to human skin (HFF-1) cells [75] and human keratinocytes HaCaT cells [76], [77]. Piao et al. demonstrated that particulate matter caused endoplasmic reticulum stress, mitochondrial damage [increase in mitochondrial depolarization (damaged state) and expression of Bax (pro-apoptotic member of the Bcl-2 family)], and autophagy [accumulation of intracellular vacuoles indicative of autophagy as well as the expression of beclin-1 (a protein that initiates autophagosome formation during autophagy) and LC3B-II (the processed form of LC3), and induced apoptotic cell death in human keratinocytes and HR-1 hairless mouse skin tissue via ROS generation [78]. ROS could also induce skin inflammation. Recently, Ryu et al. reported that particulate matter induced skin inflammation by simulating secretion of the pro-inflammatory cytokine IL-6. The expression of IL-6 was promoted via activation of NFκB signalling by interaction with the toll-like receptor 5-NADPH oxidase 4 (TLR5-NOX4), which caused ROS generation in human keratinocyte HaCaT cells and C57BL/6 J (wild type) mice skin [79]. Jin et al. also found that particulate matter caused inflammation via ROS-mediated induction of inflammatory cytokines IL-8 and matrix metalloproteinase-1 (MMP-1) in primary keratinocytes and BALB/c mouse skin [80].

6. Conclusion and future directions

The prevalence of antimicrobial resistance has resulted in the diminished efficacy of antibiotic treatments to cure a wide range of infections caused by pathogens and increased mortality rates. Health care costs for patients with resistant infections are constantly increasing due to the need for high drug

dosages, longer durations of illness, additional tests and requirements for more expensive medicines [81], [82]. Proper selection of effective dosage regimens for antimicrobial drugs and the development of novel antimicrobial agents would be very useful against antimicrobial-resistant pathogens. Furthermore, searching for useful strategies is necessary to control the widespread antimicrobial resistance due to the limited access to new antimicrobial drugs. One potentially effective strategy is to kill the pathogens via the contribution of ROS on antimicrobial lethality. When increased antimicrobial potency of ROS is observed, their potential cytotoxicity might also be increased. An ideal antimicrobial therapy using the ROS pathway should be utilized in the most proper and safe manner to destroy or kill pathogenic microorganisms and prevent or minimize cytotoxic and adverse effects in patients. To combat antimicrobial resistance, conventionally used antibiotics could be combined with compounds that accelerate ROS formation synergistically to potentiate the antimicrobial properties. Recently, synergistic antimicrobial effects of ISO with AmB or FLC [59], silver with gentamicin, kanamycin, geneticin, or tetracycline [83], and alanine with kanamycin [84] have been reported to be due to the oxidative stress caused by ROS induction. ROS could be a potent candidate when combined with conventional drugs to improve antimicrobial efficacy. Owing to the lack of novel antimicrobials and therapeutic choices, antimicrobial strategies such as ROS could be a possible strategy to deal with the urgent situation of antimicrobial resistance. ROS could be a potent tool to combat microbial infections, as ROS are toxic against a broad range of pathogens via triggering oxidative stress. The oxidative stress caused by ROS, can damage cellular macromolecules such as DNA, resulting in malfunction and eventually microbial cell death. The future development of ROS-based strategies as clinical therapies for microbial infections remains challenging, but at least some of them should become well established and sufficiently developed to reach clinical practice.

Conflict of interest statement

The authors declare no conflict of interest.

Acknowledgements

This work was supported by the Fund for State Key Laboratory of Chemical Biology and Drug Discovery and Department of Applied Biology and Chemical Technology, The Hong Kong Polytechnic University, Hong Kong SAR, PR China and a research fund from the Research and Development Division of Kamford Biotechnology Company Limited. We also thanks anonymous reviewers for critical comments and suggestions to improve the quality of our manuscript.

References

[1] Antibiotic resistance threats in the United States, 2013. USA: Centers for Disease Control and Prevention; 2013.

[2] Tackling AMR, the Antimicrobial Resistance, available in: http://www.comece.eu/tackling-amr-the-antimicrobial-resistance

[3] Global antimicrobial resistance surveillance system (GLASS) report: early implementation, 2016-2017. Geneva: World Health Organization; 2017. Licence: CC BY-NC-SA 3.0 IGO.

[4] I.A. Rather, B.C. Kim, V.K. Bajpai, Y.H. Park. Self-medication and antibiotic resistance: Crisis, current challenges, and prevention. Saudi J. Biol. Sci., 24 (2017), pp. 808-812.

[5] C.L. Ventola. The antibiotic resistance crisis: part 1: causes and threats. P T, 40 (2015), pp. 277-283.

[6] Centers for Disease Control and Prevention, Outpatient Antibiotic Prescriptions — United States, 2015 accessed July 31, 2018, https://www.cdc.gov/antibiotic-use/community/pdfs/Annual-Report-2015.pdf.

665 [7] World Health Organization, Stop using antibiotics in healthy animals to prevent the spread of
666 antibiotic resistance, accessed September 10, 2019, https://www.who.int/news-room/detail/07-11-
667 2017-stop-using-antibiotics-in-healthy-animals-to-prevent-the-spread-of-antibiotic-resistance.

668 [8] WHO guidelines on use of medically important antimicrobials in food-producing animals. Geneva:
669 World Health Organization; 2017. Licence: CC BY-NC-SA 3.0 IGO.

670 [9] World Health Organization, Food safety, accessed September 10, 2019, https://www.who.int/news-
671 room/fact-sheets/detail/food-safety.

672 [10] M. Dryden. Reactive oxygen species: a novel antimicrobial. Int. J. Antimicrob. Agents, 51 (2018), pp.
673 299-303.

674 [11] M. Dryden, J. Cooke, R. Salib, R. Holding, S.L.F. Pender, J. Brooks. Hot topics in reactive oxygen
675 therapy: antimicrobial and immunological mechanisms, safety and clinical applications. J. Glob.
676 Antimicrob. Resist., 8 (2017), pp. 194–198.

677 [12] M.S. Dryden, J. Cooke, R.J. Salib, R.E. Holding, T. Biggs, A.A. Salamat, R.N. Allan, R.S. Newby, F.
678 Halstead, B. Oppenheim, T. Hall, S.C. Cox, L.M. Grover, Z. Al-Hindi, L. Novak-Frazer, M.D. Richardson.
679 Reactive oxygen: A novel antimicrobial mechanism for targeting biofilm-associated infection. J. Glob.
680 Antimicrob. Resist., 8 (2017), pp. 186-191.

681 [13] J.H. Powers. Antimicrobial drug development – the past, the present, and the future. Clin. Microbiol.
682 Infect., 10 (2004), pp. 23-31.

683 [14] M. Dryden, X. Hudgell, K. Saeed, A.W.S. Dryden, J. Brooks, J. Cooke. Surgihoney – honey wound
684 treatment: first report of in‐vitro activity and early clinical evaluation. Birmingham, UK: Federation of
685 Infection Societies, 2013.

686 [15] J. Cooke, M. Dryden, T. Patton, J. Brennan, J. Barrett. The antimicrobial activity of prototype
687 modified honeys that generate reactive oxygen species (ROS) hydrogen peroxide. BMC Res. Notes, 8
688 (2015), pp. 20.

689 [16] M. Dryden, C. Goddard, A. Madadi, M. Heard, K. Saeed, J. Cooke. Bioengineered Surgihoney as an
690 antimicrobial wound dressing to prevent Caesarean wound infection: a clinical and cost‐effectiveness
691 study. Br. J. Midwifery, 22 (2014), pp. 23‐27.]

692 [17] M. Zuluaga, V. Gueguen, D. Letourneur, G. Pavon-Djavid. Astaxanthin-antioxidant impact on
693 excessive Reactive Oxygen Species generation induced by ischemia and reperfusion injury. Chem. Biol.
694 Interact., 279 (2018), pp.145-158.

695 [18] B. Halliwell, J.M. Gutteridge. Oxygen toxicity, oxygen radicals, transition metals and disease.
696 Biochem. J., 219 (1984), pp. 1–14.

697 [19] V.I. Lushchak. Free radicals, reactive oxygen species, oxidative stress and its classification. Chem.-
698 Biol. Interact., 224 (2014), pp. 164-175.

699 [20] T.O. Ajiboye, M. Aliyu, I. Isiaka, F.Z. Haliru, O.B. Ibitoye, J.N. Uwazie, H.F. Muritala, S.A. Bello, I.I.
700 Yusuf, A.O. Mohammed. Contribution of reactive oxygen species to (+)-catechin-mediated bacterial
701 lethality. Chem. Biol. Interact., 258 (2016), pp. 276-287.

702 [21] A.R. Phull, B. Nasir, I.U. Haq, S.J. Kim. Oxidative stress, consequences and ROS mediated cellular
703 signaling in rheumatoid arthritis. Chem. Biol. Interact., 281 (2018), pp. 121-136.

704 [22] Y. Maejima, D. Zablocki, J. Sadoshima. Chapter 23: Oxidative Stress and Cardiac Muscle. In: Hill JA
705 and Olson EN, editors. Muscle - Fundamental Biology and Mechanisms of Disease, Volume 1, Oxford:
706 Academic Press, Elsevier Inc. (2012), pp. 309-322.

[23] F. Haber, J. Weiss. The catalytic decomposition of hydrogen peroxide by iron salts. Proc. R. Soc. London Ser. A, 147 (1934), pp. 332–351.

[24] C. Walling. The Nature of the Primary Oxidants in Oxidations Mediated by Metal Ions. In: Oxidases and Related Redox Systems: Proceedings of the Third International Symposium. T.E. King, H.S. Mason, M. Morrison (Eds.), Pergamon Press, New York, 1982, pp. 85–97.

[25] J.A. Imlay. Diagnosing oxidative stress in bacteria: not as easy as you might think. Curr. Opin. Microbiol., 24 (2015), pp. 124-131.

[26] E. Cabiscol, J. Tamarit, J. Ros. Oxidative stress in bacteria and protein damage by reactive oxygen species. Int. Microbiol., 3 (2000), pp. 3–8.

[27] Z.N. Kashmiri, S.A. Mankar. Free radicals and oxidative stress in bacteria. Int. J. Curr. Microbiol. App. Sci., 3 (2014), pp. 34-40.

[28] L. Tong, C.C. Chuang, S. Wu, L. Zuo. Reactive oxygen species in redox cancer therapy. Cancer Lett., 367 (2015), pp. 18-25.

[29] M.Y. Memar, R. Ghotaslou, M. Samiei, K. Adibkia. Antimicrobial use of reactive oxygen therapy: current insights. Infect. Drug Resist., 11 (2018), pp. 567–576.

[30] A. Baez, J. Shiloach. Escherichia coli avoids high dissolved oxygen stress by activation of SoxRS and manganese-superoxide dismutase. Microb. Cell Fact., 12 (2013), pp. 23.

[31] G. Yang, Y. Bai, X. Wu, X. Sun, M. Sun, X. Liu, X. Yao, C. Zhang, Q. Chu, L. Jiang, S. Wang. Patulin induced ROS-dependent autophagic cell death in Human Hepatoma G2 cells. Chem. Biol. Interact., 288 (2018), pp. 24-31.

[32] X. Zhao, K. Drlica. Reactive oxygen species and the bacterial response to lethal stress. Curr. Opin. Microbiol., 0 (2014), pp. 1-6.

729 [33] H. Semchyshyn, T. Bagnyukova, K. Storey, V. Lushchak. Hydrogen peroxide increases the activities of
730 soxRS regulon enzymes and the levels of oxidized proteins and lipids in Escherichia coli. Cell Biol. Int., 29
731 (2005), pp. 898–902.
732 [34] F. Vatansever, W.C. de Melo, P. Avci, D. Vecchio, M. Sadasivam, A. Gupta, R. Chandran, M. Karimi,
733 N.A. Parizotto, R. Yin, G.P. Tegos, M.R. Hamblin. Antimicrobial strategies centered around reactive
734 oxygen species--bactericidal antibiotics, photodynamic therapy, and beyond. FEMS Microbiol. Rev., 37
735 (2013), pp. 955–989.
736 [35] A. Dorsey-Oresto, T. Lu, M. Mosel, X. Wang, T. Salz, K. Drlica, X. Zhao. YihE kinase is a central
737 regulator of programmed cell death in bacteria. Cell Rep., 3 (2013), pp. 528-537.
738 [36] Y. Hong, J. Zeng, X. Wang, K. Drlica, X. Zhao. Post-stress bacterial cell death mediated by reactive
739 oxygen species. PNAS, 116 (2019), pp. 10064–10071.
740 [37] M.A. Kohanski, D.J. Dwyer, B. Hayete, C.A. Lawrence, J.J. Collins. A common mechanism of cellular
741 death induced by bactericidal antibiotics. Cell, 130 (2007), pp. 797-810.
742 [38] Y. Hong, K. Drlica, X. Zhao. Antimicrobial-mediated bacterial suicide. In: Antimicrobial Resistance in
743 the 21st Century. I. Fong, D. Shlaes, K. Drlica (Eds.), Springer Press, 2018. pp. 619-642.
744 [39] M.A. Kohanski, D.J. Dwyer, J. Wierzbowski, G. Cottarel, J.J. Collins. Mistranslation of membrane
745 proteins and two-component system activation trigger antibiotic-mediated cell death. Cell, 135(2008),
746 pp. 679-690.
747 [40] X. Wang, X. Zhao. Contribution of oxidative damage to antimicrobial lethality. Antimicrob. Agents
748 Chemother., 53 (2009), pp. 1395-1402.
749 [41] R.M. Burger, K. Drlica. Superoxide protects Escherichia coli from bleomycin mediated lethality. J.
750 Inorg. Biochem., 103 (2009), pp. 1273-1277.

751 [42] Mosel M, Li L, Drlica K, Zhao X. 2013. Superoxide-mediated protection of Escherichia coli from
752 antimicrobials. Antimicrob Agents Chemother 57:5755–5759.

753 [43] J.J. Foti, B. Devadoss, J.A. Winkler, J.J. Collins, G.C. Walker. Oxidation of the guanine nucleotide pool
754 underlies cell death by bactericidal antibiotics. Science 336 (2012), pp. 315–319.

755 [44] I. Keren, Y. Wu, J. Inocencio, L.R. Mulcahy, K. Lewis. Killing by bactericidal antibiotics does not
756 depend on reactive oxygen species. Science, 339 (2013), pp. 1213–1216.

757 [45] Y. Liu, J.A. Imlay. Cell death from antibiotics without the involvement of reactive oxygen species.
758 Science, 339 (2013), pp. 1210–1213.

759 [46] D.J. Dwyer, J.J. Collins, G.C. Walker. Unraveling the physiological complexities of antibiotic lethality.
760 Annu. Rev. Pharmacol. Toxicol., 55 (2015), pp. 313-332.

761 [47] X. Zhao, Y. Hong, K. Drlica. Moving forward with reactive oxygen species involvement in
762 antimicrobial lethality. J. Antimicrob. Chemother., 70 (2015), pp. 639-642.

763 [48] M. Malik, S. Hussain, K. Drlica. Effect of anaerobic growth on quinolone lethality with Escherichia
764 coli. Antimicrob. Agents Chemother., 51 (2007), pp. 28–34.

765 [49] M. Malik, G. Hoatam, K. Chavda, R. J. Kerns, K. Drlica. Novel approach for comparing abilities of
766 quinolones to restrict the emergence of resistant mutants during quinolone exposure. Antimicrob.
767 Agents Chemother., 54 (2010), pp. 149–156.

768 [50] D.J. Dwyer, P.A. Belenky, J.H. Yang, I.C. MacDonald, J.D. Martell, N. Takahashi, C.T. Chan, M.A.
769 Lobritz, D. Braff, E.G. Schwarz, J.D. Ye, M. Pati, M. Vercruysse, P.S. Ralifo, K.R. Allison, A.S. Khalil, A.Y.
770 Ting, G.C. Walker, J.J. Collins. Antibiotics induce redox-related physiological alterations as part of their
771 lethality. Proc. Natl. Acad. Sci. U S A. 111 (2014), pp. E2100-9.

772 [51] P. Belenky, J.D. Ye, C.B. Porter, N.R. Cohen, M.A. Lobritz, T. Ferrante, S. Jain, B.J. Korry, E.G. Schwarz,
773 G.C. Walker, J.J. Collins. Bactericidal Antibiotics Induce Toxic Metabolic Perturbations that Lead to
774 Cellular Damage. Cell Rep., 13 (2015), pp. 968-980.

775 [52] P.J. Bassford Jr, T.J. Silhavy, J.R. Beckwith. Use of gene fusion to study secretion of maltose-binding
776 protein into Escherichia coli periplasm. J. Bacteriol., 139 (1979), pp. 19–31.

777 [53] E. Brickman, T.J. Silhavy, P.J. Bassford Jr, H.A. Shuman, J.R. Beckwith. Sites within gene lacZ of
778 Escherichia coli for formation of active hybrid beta-galactosidase molecules. J. Bacteriol., 139 (1979), pp.
779 13–18.

780 [54] N. Takahashi, C.C. Gruber, J.H. Yang, X. Liu, D. Braff, C.N. Yashaswini, S. Bhubhanil, Y. Furuta, S.
781 Andreescu, J.J. Collins, G.C. Walker. Lethality of MalE-LacZ hybrid protein shares mechanistic attributes
782 with oxidative component of antibiotic lethality. Proc. Natl. Acad. Sci. U S A., pii (2017), pp. 201707466.

783 [55] Y. Hong, L. Li, G. Luan, K. Drlica, X. Zhao. Contribution of reactive oxygen species to thymineless
784 death in Escherichia coli. Nat Microbiol. 2017 Dec;2(12):1667-1675.

785 [56] G. Luan, Y. Hong, K. Drlica, X. Zhao. Suppression of Reactive Oxygen Species Accumulation Accounts
786 for Paradoxical Bacterial Survival at High Quinolone Concentration. Antimicrob. Agents Chemother., 62
787 (2018), pp. e01622-17.

788 [57] K.S. Ong, Y.L. Cheow, S.M. Lee. The role of reactive oxygen species in the antimicrobial activity of
789 pyochelin. J. Adv. Res., 8 (2017), pp. 393-398.

790 [58] S. Kim, D. Gun Lee. Role of calcium in reactive oxygen species-induced apoptosis in Candida albicans:
791 An antifungal mechanism of antimicrobial peptide, PMAP-23. Free Radic. Res., 53 (2019), pp. 8-17.

792 [59] S. Kim, E.R. Woo, D.G. Lee. Synergistic Antifungal Activity of Isoquercitrin: Apoptosis and Membrane
793 Permeabilization Related to Reactive Oxygen Species in Candida albicans. IUBMB Life, 71 (2019), pp.
794 283-292.

795 [60] W. Lee, E.R. Woo, D.G. Lee. Effect of apigenin isolated from Aster yomena against Candida albicans:
796 apigenin-triggered apoptotic pathway regulated by mitochondrial calcium signalling. J. Ethnopharmacol.,
797 231 (2019), pp. 19-28.

798 [61] J.T.A. Oliveira, P.F.N. Souza, I.M. Vasconcelos, L.P. Dias, T.F. Martins, M.F. Van Tilburg, M.I.F. Guedes,
799 D.O.B. Sousa. Mo-CBP3-PepI, Mo-CBP3-PepII, and Mo-CBP3-PepIII are synthetic antimicrobial peptides
800 active against human pathogens by stimulating ROS generation and increasing plasma membrane
801 permeability. Biochimie, 157 (2019), pp. 10-21.

802 [62] L. Hu, H. Wang, T. Xia, B. Fang, Y. Shen, Q. Zhang, X. Tian, H. Zhou, J. Wu, Y. Tian. Two-Photon-Active
803 Organotin(IV) Complexes for Antibacterial Function and Superresolution Bacteria Imaging. Inorg. Chem.,
804 57 (2018), pp. 6340-6348.

805 [63] N.D. Savić, S. Vojnovic, B.Đ. Glišić, A. Crochet, A. Pavic, G.V. Janjić, M. Pekmezović, I.M. Opsenica,
806 K.M. Fromm, J. Nikodinovic-Runic, M.I. Djuran. Mononuclear silver(I) complexes with 1,7-phenanthroline
807 as potent inhibitors of Candida growth. Eur. J. Med. Chem., 156 (2018), pp. 760-773.

808 [64] Z. Song, H. Wang, Y. Wu, J. Gu, S. Li, H. Han. Fabrication of Bis-Quaternary Ammonium Salt as an
809 Efficient Bactericidal Weapon Against Escherichia coli and Staphylococcus aureus. ACS Omega, 3 (2018),
810 pp. 14517-14525.

811 [65] L. Wang, S. Monro, P. Cui, H. Yin, B. Liu, C.G. Cameron, W. Xu, M. Hetu, A. Fuller, S.V. Kilina, S.A.
812 McFarland, W. Sun. Heteroleptic Ir(III)N6 complexes with long-lived triplet excited states and in vitro
813 photobiological activities. ACS Appl. Mater. Interfaces, 11 (2019), pp. 3629-3644.

814 [66] H. Liu, X. Qu, E. Kim, M. Lei, K. Dai, X. Tan, M. Xu, J. Li, Y. Liu, X. Shi, P. Li, G.F. Payne, C. Liu. Bio-
815 inspired redox-cycling antimicrobial film for sustained generation of reactive oxygen species.
816 Biomaterials, 162 (2018), pp. 109-122.

817 [67] Z. Wang, H. Bai, C. Lu, C. Hou, Y. Qiu, P. Zhang, J. Duan, H. Mu. Light controllable chitosan micelles
818 with ROS generation and essential oil release for the treatment of bacterial biofilm. Carbohydr. Polym.
819 205 (2019), pp. 533-539.

820 [68] O. Antonoglou, K. Giannousi, J. Arvanitidis, S. Mourdikoudis, A. Pantazaki, C. Dendrinou-Samara.
821 Elucidation of one step synthesis of PEGylated CuFe bimetallic nanoparticles. Antimicrobial activity of
822 CuFe@PEG vs Cu@PEG. J. Inorg. Biochem., 177 (2017), pp. 159-170.

823 [69] V.T. Anju, P. Paramanantham, S.L. Sruthil, A. Sharan, M.H. Alsaedi, T.M.S. Dawoud, A. Syed, B.
824 Siddhardha. Antimicrobial photodynamic activity of rose bengal conjugated multi walled carbon
825 nanotubes against planktonic cells and biofilm of Escherichia coli. Photodiagnosis Photodyn. Ther., 24
826 (2018), pp. 300-310.

827 [70] G. Vitiello, A. Zanfardino, O. Tammaro, M.D. Napoli, M.F. Caso, A. Pezzella, M. Varcamonti, B.
828 Silvestri, G. D'Errico, A. Costantini, G. Luciani. Bioinspired hybrid eumelanin–TiO2 antimicrobial
829 nanostructures: the key role of organo–inorganic frameworks in tuning eumelanin's biocide action
830 mechanism through membrane interaction. RSC Adv., 8 (2018), pp. 28275–28283.

831 [71] H.F. Khalid, B. Tehseen, Y. Sarwar, S.Z. Hussain, W.S. Khan, Z.A. Raza, S.Z. Bajwa, A.G. Kanaras, I.
832 Hussain, A. Rehman. Biosurfactant coated silver and iron oxide nanoparticles with enhanced anti-biofilm
833 and anti-adhesive properties. J. Hazard Mater., 364 (2019), pp. 441-448.

834 [72] A. Nastulyavichus, S. Kudryashov, N Smirnov, I. Saraeva, A. Rudenko, E. Tolordava, A. Ionin, Y.
835 Romanova, D. Zayarny. Antibacterial coatings of Se and Si nanoparticles. Appl. Surf. Sci., 469 (2019), pp.
836 220-225.

837 [73] P. Parasuraman, V.T. Anju, S.B. Sruthil Lal, A. Sharan, S. Busi, K. Kaviyarasu, M. Arshad, T.M.S.
838 Dawoud, A. Syed. Synthesis and antimicrobial photodynamic effect of methylene blue conjugated
839 carbon nanotubes on E. coli and S. aureus. Photochem. Photobiol. Sci., 18 (2019), pp. 563-576.

840 [74] S. Pillai, C. Oresajo, J. Hayward. Ultraviolet radiation and skin aging: roles of reactive oxygen species,
841 inflammation and protease activation, and strategies for prevention of inflammation-induced matrix
842 degradation - a review. Int. J. Cosmet. Sci., 27 (2005), pp. 17–34.

843 [75] P. Ghaderi-Shekhi Abadi, F.H. Shirazi, M. Joshaghani, H.R. Moghimi. Influence of formulation of ZnO
844 nanoblokes containing metallic ions dopants on their cytotoxicity and protective factors: An in vitro
845 study on human skin cells exposed to UVA radiation. Toxicol. Rep., 5 (2018), pp. 468–479.

846 [76] D. Ali, A. Tripathi, H. Al Ali, Y. Shahi, K.K. Mishra, S. Alarifi, A.A. Alkahtane, S. Manohardas. ROS-
847 dependent Bax/Bcl2 and caspase 3 pathway-mediated apoptosis induced by zineb in human
848 keratinocyte cells. Onco. Targets Ther., 11 (2018), pp. 489–497.

849 [77] L. Li, T. Huang, C. Lan, H. Ding, C. Yan, Y. Dou. Protective effect of polysaccharide from Sophora
850 japonica L. flower buds against UVB radiation in a human keratinocyte cell line (HaCaT cells). J.
851 Photochem. Photobiol. B, 191 (2019), pp. 135-142.

852 [78] M.J. Piao, M.J. Ahn, K.A. Kang, Y.S. Ryu, Y.J. Hyun, K. Shilnikova, A.X. Zhen, J.W. Jeong, Y.H. Choi, H.K.
853 Kang, Y.S. Koh, J.W. Hyun. Particulate matter 2.5 damages skin cells by inducing oxidative stress,
854 subcellular organelle dysfunction, and apoptosis. Arch. Toxicol., 92 (2018), pp. 2077-2091.

855 [79] Y.S. Ryu, K.A. Kang, M.J. Piao, M.J. Ahn, J.M. Yi, Y.M. Hyun, S.H. Kim, M.K. Ko, C.O. Park, J.W. Hyun.
856 Particulate matter induces inflammatory cytokine production via activation of NFκB by TLR5-NOX4-ROS
857 signaling in human skin keratinocyte and mouse skin. Redox Biol., 21 (2019), pp. 101080.

858 [80] S.P. Jin, Z. Li, E.K. Choi, S. Lee, Y.K. Kim, E.Y. Seo, J.H. Chung, S. Cho. Urban particulate matter in air
859 pollution penetrates into the barrier-disrupted skin and produces ROS-dependent cutaneous
860 inflammatory response in vivo. J. Dermatol. Sci., 91 (2018), pp. 175-183.

861 [81] WHO report on surveillance of antibiotic consumption: 2016-2018 early implementation. Geneva:
862 World Health Organization; 2018. Licence: CC BY-NC-SA 3.0 IGO.

863 [82] P.L. Lam, K.K.H. Lee, R.S.M. Wong, G.Y.M. Cheng, Z.X. Bian, C.H. Chui, R. Gambari. Recent advances
864 on topical antimicrobials for skin and soft tissue infections and their safety concerns. Crit. Rev.
865 Microbiol., 44 (2018), pp. 40-78.

866 [83] L. Zou, J. Wang, Y. Gao, X. Ren, M.E. Rottenberg, J. Lu, A. Holmgren. Synergistic antibacterial activity
867 of silver with antibiotics correlating with the upregulation of the ROS production. Sci. Rep., 8 (2018), pp.
868 11131.

869 [84] J.Z. Ye, Y.B. Su, X.M. Lin, S.S. Lai, W.X. Li, F. Ali, J. Zheng, B. Peng. Alanine Enhances Aminoglycosides-
870 Induced ROS Production as Revealed by Proteomic Analysis. Front Microbiol., 9 (2018), pp. 29.